In vitro evaluation of NA1-115-7-loaded nanoemulsions, an MCL-1-specific inhibitor of natural origin, intended to treat B-cell lymphoproliferative disorders after oral administration

Line Séguy, Florian Daressy, Sophia Lahlil, Sophie Corvaisier, Vincent Dumontet, Marc Litaudon, Cécile Apel, Fanny Roussi, Joëlle Wiels, Aude Robert, et al.

In vitro evaluation of NA1-115-7-loaded nanoemulsions, an MCL-1-specific inhibitor of natural origin, intended to treat B-cell lymphoproliferative disorders after oral administration

Line Séguy, Florian Daressy, Sophia Lahlil, Sophie Corvaisier, Vincent Dumontet, Marc Litaudon, Cécile Apel, Fanny Roussi, Joëlle Wiels, Aude Robert, et al.

In vitro evaluation of NA1-115-7-loaded nanoemulsions, an MCL-1-specific inhibitor of natural origin, intended to treat B-cell lymphoproliferative disorders after oral administration

Line Séguy [a, 1], Florian Daressy [b, c, 1], Sophia Lahlil [c], Sophie Corvaisier [a], Vincent Dumontet [b], Marc Litaudon [b], Cécile Appel [b], Fanny Roussi [b], Joëlle Wiels [c], Aude Robert [d], Anne-Claire Groo [a, *], Aurélie Malzert-Fréon [a]

[a] *Normandie Univ, UNICAEN, CERMN, 14000 Caen, France*
[b] *Institut de Chimie des Substances Naturelles, CNRS, UPR2301, Université Paris-Saclay, 91198 Gif-sur-Yvette, France*
[c] *UMR 9018 CNRS, Université Paris-Saclay, Gustave Roussy, 94805 Villejuif, France*
[d] *UMR1279 INSERM, Université Paris-Saclay, Gustave Roussy, 94805 Villejuif Cedex, France*

A B S T R A C T

MCL-1, an anti-apoptotic member of the BCL-2 protein family, is overexpressed in many types of cancer and contributes to chemotherapy resistance. The drimane derivative NA1-115-7 is a natural compound isolated from *Zygogynum pancheri* that can be considered as a very promising lead for treating MCL-1-dependent hematological malignancies. As this drug suffers from low stability in acidic conditions and poor aqueous solubility, we evaluated the potential oral use of NA1-115–7 by encapsulating it in lipid nanoemulsions (NA-NEs) prepared by spontaneous emulsification. NA-NEs showed a particle size of 41.9 ± 2.2 nm, PDI of 0.131 ± 0.016, zeta potential of –5.8 ± 3.4 mV, encapsulation efficiency of approximately 100 % at a concentration of 24 mM. The stability of NA-1–115–7 was sixfold higher than that of the unencapsulated drug in simulated gastric fluid. NA-NEs significantly restored apoptosis and halved the effective doses of NA1-115–7 on BL2, a Burkitt lymphoma cell line, without toxicity in normal cells. Such a drug-delivery system appears to be particularly interesting for the oral administration of NA1-115–7, as it improves its solubility and stability, as well as efficacy, by reducing the therapeutic dose, making it possible to further consider in-vivo studies of this promising drug in BL2 xenografted mice.

1. Introduction

Proteins of the BCL-2-family are key regulators of apoptosis. In many types of cancer, in particular, hematological cancers, the expression of BCL-2 family proteins is dysregulated in favor of anti-apoptotic proteins. Among them, MCL-1 has emerged as a promising target for new therapies. Indeed, overexpression of the MCL-1 protein has been shown to correlate with tumorigenesis (Campbell et al., 2010) and tumor maintenance (Glaser et al., 2012). Over the last several years, synthetic inhibitors targeting MCL-1 and belonging to BH3-mimetics have been developed. By mimicking the BH3-domain, a region essential for interactions between members of the BCL-2 protein family (Letai et al., 2002), these small molecules bind to the hydrophobic groove of MCL-1, liberating the pro-apoptotic proteins, thus restoring apoptosis and inducing the death of cancer cells (Delbridge and Strasser, 2015). The efficacy of several synthetic molecules acting as MCL-1 inhibitors has been demonstrated in preclinical studies when used alone or in combination with other drugs (Bhagwat et al., 2021; Caenepeel et al., 2018; Hedir et al., 2018; Kotschy et al., 2016; Ramsey et al., 2018; Tron et al., 2018).

NA1-115–7, a natural product isolated from *Zygogynum ancheri*, is a promising new selective inhibitor of MCL-1 (Daressy et al., 2021). NMR and MALDI data have shown that NA1-115–7 is able to bind to MCL-1 in the BH3 binding groove and form a covalent bond with a lysine *via* the formation of a Paal-Knorr pyrrole adduct. NA1-115–7 can therefore be considered as the first covalent BH3-mimetic that targets MCL-1. It could act as a "suicide" molecule; once bound to its target, it is degraded with it. *In-vitro* evaluation confirmed that, at micromolar doses, NA1-115–7 acts as a true BH3-mimetic, capable of disrupting the BAK/MCL-1 interaction and consequently, capable of activating BAX/BAK-dependent apoptosis, leading to the rapid and specific death of MCL-1-dependent cells. Interestingly, MCL-1-dependent hematological cell lines, such as BL2, were shown to be efficiently killed by NA1-115–7,

* Corresponding author.
E-mail address: anne-claire.groo@unicaen.fr (A.-C. Groo).
[1] Equal contribution.

and the compound was not cardiotoxic at doses that induced tumor cell apoptosis (Daressy et al., 2021, 2022).

However, as many natural compounds, NA1-115–7 has a lipophilic structure (estimated logP of 3.50 from ChemAxon software), which may hinder its *in-vivo* evaluation (Fomekong Fotsop et al., 2008). The drugability parameters of this lead could therefore hinder its preclinical development and its sensitivity to acidic conditions could equally hinder its oral administration and, thus, clinical development (Daressy et al., 2022). It is, therefore, crucial to find a strategy to improve its solubility and stability.

Among formulation strategies that can be proposed to reach the preclinical stage, certain drug-delivery systems may be advantageous. Indeed, nanocarriers can protect active pharmaceutical ingredients from degradation, increase their absorption by facilitating diffusion across the epithelium, modify the pharmacokinetics and tissue distribution profile of a drug, and/or improve intracellular penetration and distribution (Couvreur and Vauthier, 2006). The use of lipid-based nanomedicines has proven to be particularly advantageous in cancer treatment by improving the activity of several drugs (García-Pinel et al., 2019). For example, lipid nanoemulsions enabled a 1,000-fold increase in the apparent solubility of pyridoclax, an MCL-1 inhibitor, and showed improved cytotoxic activity relative to the free drug (Hedir et al., 2018; Groo et al., 2020).

On the basis of the biocompatibility profile of excipients assessed in a miniaturized hemolytic test and experimental work, our team has recently developed lipid NEs generated from a simple formulation process by self-emulsification (Séguy et al., 2020). Their advantages include high temporal stability and high loading capacity. This formulation appeared to be highly efficient in improving the apparent solubility of well-known anticancer drugs, without the use of any organic solvents, and can be proposed for their biological study (Ceramella et al., 2021).

Here, in anticipation of the preclinical evaluation of the new lead NA1-115–7 and considering that the oral route is the most common and convenient route of administration in animals, we first characterized the stability of the drug in biomimetic media adapted to oral administration. Then, to improve its drugability parameters, we developed NA1-115–7-loaded nanoemulsions. The toxicity of this new formulation of NA1-115–7 was determined on normal cells, as well as its activity against lymphoproliferation cells. Both were compared to the unencapsulated drug.

2. Materials and methods

2.1. Materials

Kolliphor® HS15 (macrogol 15 hydroxystearate: 70 % PEG 660 hydroxystearate and 30 % free PEG 660) was kindly provided by BASF (Ludwigshafen, Germany). Labrafac® WL 1349 (medium-chain triglyceride) and Transcutol® HP (diethylene glycol monoethyl ether) were gifts from Gattefosse S.A. (Saint-Priest, France). Due to the complex composition of the excipients, the brand names are used in the text. $Na_2HPO_4{\cdot}12H_2O$, KH_2PO_4, KCl, $MgCl_2$, propidium iodide, pepsin from porcine gastric mucosa, sodium taurocholate hydrate, 1-oleoyl-*rac*-glycerol, sodium oleate, maleic acid, and pancreatin (>3 × USP specification) were purchased from Merck (Steinheim, Germany). Lipoid E PC (Phosphatidyl choline from egg lecithin) was a gift from Lipoid GmbH (Ludwigshafen, Germany). $CaCl_2$ was purchased from Prolabo VWR International (Fontenay-sous-Bois, France). NaCl was purchased from Acros Organics (Geel, Belgium). Water, methanol, and acetonitrile of HPLC analytical grade were purchased from Fisher Scientific (Loughborough, United Kingdom). The demineralized water used was obtained using a mixed bed ion exchange resin Distiplus DS450 (Grosseron, Couëron, France). DMSO was purchased from Fisher Scientific (Illkirch, France).

The BL2 and Remb1 cell lines were purchased from the International Agency for Research on Cancer (IARC, Lyon, France). All cell lines were cultured in RPMI 1640 medium (Fisher Scientific, Illkirch, France) containing 1 mM sodium pyruvate, 2 mM L-glutamine, 20 mM glucose, 100 µg/mL streptomycin, 100 U/mL penicillin, and 10 % heat-inactivated fetal calf serum (complete RPMI medium). Cell lines were maintained at 37 °C in a humidified atmosphere containing 5 % CO_2.

2.2. Plant material and obtention of pure NA1-115–7

Trunk bark and leaves of *Z. pancheri* subspecies *pancheri* were collected in the Nodela rainforest (South Province of New Caledonia) by one of the authors (V.D.). The corresponding reference specimen (DUM-578) is kept at the Herbarium of New Caledonia (NOU). The extraction and isolation of NA1-115–7 were performed according to a previously described procedure (Allouche et al., 2009). This compound was identified by spectroscopic methods (^{1}H NMR, ^{13}C NMR, IR, UV, and mass) and by comparison with data reported in the literature (Larsen et al., 2007).

2.3. NA1-115–7 characterization

2.3.1. Thermodynamic solubility determination at pH 7.4

The thermodynamic solubility of NA1-115–7 was determined in a phosphate-buffered saline solution at pH 7.4 using a miniaturized shake-flask procedure as previously reported by our group (Groo et al., 2017). Briefly, 10 µL of a 50 mM solution of NA1-115–7 solubilized in DMSO was added to 990 µL buffer solution in a 5 mL glass tube (n = 4). Immediate precipitation was observed in the tubes. After shaking at room temperature by inversion for 24 h, the solution was transferred to microtubes and centrifuged at 14,500 × g for 5 min. Then, 100 µL supernatant was mixed with 100 µL acetonitrile/DMSO (99:1; v/v) in a 96-well UV plate (Greiner Bio-One, Frickenhausen, Germany). Determination of the solubility was performed using an Infinite M200 plate reader (Tecan, Männedorf, Switzerland) in spectrophotometric mode (λ^{max} = 280 nm). Quantitative analyses were performed using a linear calibration curve (R^2 > 0.999) of seven standard solutions (0, 2, 5, 10, 20, 50, and 100 µM) of NA-115–7 solubilized in a 50:50 (v/v) mixture of buffer with acetonitrile/DMSO (99:1; v/v).

2.3.2. Gastrointestinal tract parallel artificial membrane permeability (PAMPA-GIT) assays

PAMPA-GIT experiments were performed using the PAMPA Explorer Kit (Pion Inc., Billerica, MA, USA) according to the manufacturer's protocol. Briefly, NA-115–7 was dissolved in DMSO to form a 10 mM stock solution. This solution was then diluted 1/200 (v/v) in Prisma HT buffer at pH 6.0 or pH 5.0 and 200 µL added to the donor plates (n = 4). Each membrane filter of the acceptor plate (P/N 110243) was coated with 5 µL GIT-0 Lipid (P/N 110669) and each acceptor well filled with 200 µL acceptor sink buffer (P/N 110139). After 4 h of incubation at room temperature without stirring, the sandwich was separated and the amounts of NA-115–7 in the donor and acceptor compartments quantified by UV–visible spectrometry using an Infinite M200 microplate reader (Tecan, Männedorf, Switzerland). The permeability value (Pe) was calculated using PAMPA Explorer software version 3.7 (pION). The control standards for the PAMPA-GIT experiment were ketoprofen (with a Pe of 648.1 ± 114.0 nm/s at pH 5.0, 317.6 ± 19.8 nm/s at pH 6.0, and 43.5 ± 2.8 nm/s at pH 7.4) for pH-dependent permeability and antipyrine (with a Pe of 22.6 ± 0.5 nm/s at pH 5.0, 20.5 ± 5.1 nm/s at pH 6.0 and 20.4 ± 0.1 nm/s at pH 7.4) for low permeability.

2.3.3. Calculated physicochemical properties of NA

The molecular weight, pKa, and logP were calculated using standard tools of the ChemAxon Package (Marvin 19.1.0, 2019, ChemAxon (https://www.chemaxon.com)).

2.4. Formulation of the NEs

The formulation of the NEs was based on the spontaneous nanoemulsification method previously described by our group (Gué et al., 2016) and adapted by Séguy et al. (Séguy et al., 2020). Triglycerides (Labrafac® WL 1349, 84.7 mg), surfactant (Kolliphor® HS 15, 133.1 mg), and solubilizer (Transcutol® HP, 24.2 mg) were mixed, heated to 70 °C under gentle magnetic stirring (250 rpm) for 2 min, and cooled to 25 °C over 5 min, during which the magnetic stirring was increased to 750 rpm. Then, 1 mL of water was rapidly added, resulting in spontaneous emulsification. Stirring was maintained for 15 min at room temperature. NA1-115–7-loaded NEs (NA-NEs) were prepared similarly as the unloaded NEs by adding NA1-115–7, at a defined loading rate (from 1 to 4.9 % by weight), at the beginning of the formulation in the anhydrous phase. Each formulation was then filtered through 0.2 µm regenerated cellulose syringe filters (Minisart® Syringe Filter, Sartorius, Goettingen, Germany).

2.5. Granulometric properties and zeta-potential measurements

Dynamic light scattering (DLS) was used to determine the granulometric properties of the NEs in terms of mean hydrodynamic diameter and polydispersity index (PDI). A Zetasizer Ultra® apparatus (Malvern Instruments, Worcestershire, UK) equipped with a 633 nm laser at a fixed scattering angle of 173° was used. The cell temperature was kept constant at 25 °C. The NEs were diluted 1:100 (v/v) in a 1 mM NaCl solution to ensure the appropriate scattering intensity in the detector before measurements. The zeta-potential analyses were performed under the same conditions using the same apparatus equipped with a DTS 1070 cell at 25 °C, with a dielectric constant of 78.5, a refractive index of 1.33, a viscosity of 0.8872 cP, and a cell voltage of 150 V. The zeta potential was calculated from the electrophoretic mobility using the Smoluchowski equation. All measurements were performed in triplicate.

2.6. NA1-115–7 concentration measurements by HPLC

NA1-115–7 concentrations were measured by high-performance liquid chromatography (HPLC). The apparatus consisted of an Agilent 1290 binary pump, a 1290 autosampler, and a 1290 diode array UV detector (Agilent Technologies, Santa Clara, CA, USA). A C18 reversed-phase column (Restek® Ultra, 5 µm, 2.1 × 50 mm) was used. The injected volume was 8 µL and total run time 2.5 min. The flow rate was 0.5 mL/min. The temperature of the column was maintained at 25 °C. The mobile phase was initially composed of a mixture of 50 % acetonitrile (A) and 50 % water (B). A linear gradient was then applied over 2 min to reach 90 % A after 2 min, which was maintained for 0.5 min, before returning to the initial conditions. The retention time for NA1-115–7 was 1.31 min and the detection wavelength 280 nm.

Under these conditions, linearity was observed in the range of 1–100 µg/mL, with a correlation coefficient > 0.999 (y = 13.50x + 1.944). The detection and quantification limits were 0.55 and 1.62 µM, respectively. These limits were evaluated using the standard deviation of the response and the slope of calibration curve according to ICH Q2(R1) standards (International Conference on Harmonisation (ICH) of Technical Requirements for Registration of Pharmaceuticals for Human Use, 2005). In addition, the precision and accuracy of the method were evaluated by calculating the relative standard deviation (RSD) and relative errors (RE) of six inter-batch samples at low, medium, and high concentrations (Table 1). Concentrations of 2.5, 20, and 50 µg/mL were selected to avoid the extrapolation effect. The method was considered precise and accurate as the RSD and RE of all concentrations were below 15 % (González et al., 2014; Anjani et al., 2022).

Table 1
Inter-batch precision and accuracy of NA1-115–7 samples (n = 6, means ± SD).

Theoretical concentration (µg/mL)	Measured concentration (µg/mL)	Precision (%RSD)	Accuracy (%RE)
2.5	2.46 ± 0.05	2.05	1.95
20	20.13 ± 0.28	1.37	1.07
50	50.15 ± 0.51	1.02	0.74

After checking for the absence of interactions between the NEs and NA1-115–7 peaks, the HPLC method described above was also used for the NA-NEs. The NA-NE samples were first diluted in an acetonitrile/water (1:1, v/v) mixture (1/1000, v/v) and the concentration of NA1-115–7 determined.

The encapsulation efficiency (EE) was determined in triplicate and calculated as follows:

$$EE(\%) = 100 \times \frac{Quantity\ of\ NA1-115-7\ entrapped}{Total\ quantity\ of\ NA1-115-7\ added}$$

Drug loading (DL) was defined as:

$$DL(\%) = 100 \times \frac{Quantity\ of\ NA1-115-7\ entrapped}{Total\ quantity\ of\ anhydrous\ excipients}$$

2.7. Stability studies in biorelevant media

Simulated gastric fluid (SGF) was prepared according to USP XXIV (US.Pharmacopeia.XXIV, 2006) and contained 0.32 % (w/v) pepsin at a pH of 1.2. The FaSSIF/FeSSIF media are a simplification of the composition of the proximal small intestine composition in the fasted (FaSSIF) or fed states (FeSSIF). The composition of each medium used has been described before by our group (Groo et al., 2017). They were used in an updated version (V2) according to those proposed by Jantratid et *al.* (Jantratid et al., 2008), with controlled amounts of lecithin, bile components (containing bile salt and lipolysis products), and a defined pH (6.5 for FaSSIF and 5.8 for FeSSIF).

Before the stability assays of NA1-115–7, the compound was dissolved in DMSO at 10.1 mM (4.0 mg/mL). The NA1-115–7 solution and NA-NEs were diluted to a final concentration of 1 % (v/v) and incubated at 37 °C for 3 h in the various biomimetic media in triplicate. Under these conditions, the expected final concentrations in the various media were 101.7 ± 1.0 µM for NA1-115–7 and 101.9 ± 3.1 µM for the NA-NEs. Samples were taken at defined time points (0, 30, and/or 60, 120, and 180 min) and then centrifuged for 5 min at 19,980 × g to remove aggregates of the media components and precipitated NA1-115–7. Quantification of the solubilized drug in the media samples was performed by HPLC after a 1:5 dilution of the supernatant in acetonitrile and water (1/500, v/v), as described in 2.6. NA1-115–7 concentration measurements by HPLC. The granulometric characteristics of the NA-NE supernatants were measured by DLS as described in 2.5. Granulometric properties and zeta-potential measurements.

2.8. Storage stability studies

The short-term stability of the NEs was studied during a three-week storage period at 4 °C. Formulations of NA-NEs were diluted 1:100 (v/v) in 1 mM NaCl at regular intervals to evaluate the size distribution and zeta potential. In parallel, the encapsulation efficiency was quanti-

fied by the HPLC method described above. All tests and measurements were performed in triplicate.

2.9. MTT assay

The viability of BL2 cells was measured by the MTT (3-(4, 5-dimethylthiazolyl-2)-2, 5-diphenyltetrazolium bromide) assay. Cells ($7x10^4$, in triplicate) were incubated for 24 h at 37 °C with various concentrations of unloaded (i.e., blank) NEs after dilution in RPMI medium by a factor of 1:8;000 to 1:500, v/v (equivalent to 30.1 to 482.5 μg/mL of anhydrous excipients, respectively) or with equivalent concentrations of each excipient of the NEs (Kolliphor® HS15, Labrafac® WL 1349, Transcutol® HP). Next, 20 μL of MTT reagent (final concentration 1 mg/mL) was added and the plates were incubated for a further 2 h at 37 °C. Finally, 100 μL lysis buffer (30 % SDS, 33 % dimethylformamide, 2 % glacial acetic acid, 0.025 N HCl, pH = 4.7) was added and the absorbance was recorded at 570 nm after overnight incubation at room temperature. Lethal concentration 50 (LC_{50}) values were calculated after plotting the dose–response curves using GraphPad Prism software. The experiments were performed in triplicate.

2.10. Isolation of peripheral blood mononuclear cells

Peripheral blood mononuclear cells (PBMCs) were isolated on Ficoll density gradients of blood diluted in sterile PBS (1:1), as previously described (Daressy et al., 2022). Ficoll was added to the bottom of a tube and gently covered with diluted blood (1:2.5) before centrifugation at 900*g* without the brake for 20 min at room temperature. The cells at the interface (containing PBMCs) were then washed in PBS and centrifuged twice at 300*g* for 10 min. Finally, the pellet was resuspended in RPMI 1640 supplemented with 10 % FBS and cultured at 37 °C in a humidified incubator with a 5 % CO_2 atmosphere for up to 48 h.

2.11. Quantification of apoptosis

Apoptosis was assessed by labelling cells with annexin-V-FITC and propidium iodide (PI), as previously described (Daressy et al., 2022; Robert et al., 2020). Cells ($3x10^5$) were treated for the indicated times in the complete corresponding medium, washed in PBS, resuspended in annexin buffer (10 mM HEPES/NaOH, pH = 7.4, 150 mM NaCl, 5 mM KCl, 1 mM $MgCl_2$, 1.8 mM $CaCl_2$) containing 2.5 μg/mL annexin V-FITC (eBioscience) and incubated for 5 to 10 min before the addition of 100 μL annexin buffer supplemented with PI (10 μg/mL). The analyses (n = 10,000) were performed by flow cytometry (Accuri C6 cytometer, Becton, Dickinson and Company, Franklin Lakes, NJ, USA). Annexin V-positive cells (PI negative and positive) were considered to be apoptotic. For PBMCs, the cells were labelled with anti-CD3-FITC (BD Pharmingen, BD Biosciences, Franklin Lakes, NJ, USA) to identify the isolated population and with annexin V-APC. Experiments were performed at least four times.

2.12. Statistical analysis

The data were analysed using GraphPad® Prism statistical software (version 6.01, GraphPad® Software, La Jolla, CA, USA) and are expressed as means and standard deviations (SDs).

Unpaired Student's t-tests were used when two groups were analyzed and the data were normally distributed. One-way ANOVA was used for multiple comparisons of paired samples for quantitative analysis of NA-115–7 for all time points. If the results were statistically different, Tukey's post-test was performed to determine which groups were statistically different. Normality tests were performed to ensure that the data were normally distributed. For non-normally distributed data, Friedman's test, followed by Tukey's test when appropriate, was used to compared paired samples.

For cell-based assays, statistical analyses were performed using two nonparametric tests: either the Mann-Whitney test for two groups or the Kruskal–Wallis and Dunn's test for multiple comparisons.

Values of $p < 0.05$ were considered significant for all comparisons.

3. Results

3.1. NA1-115–7 solubility and stability assessment

Based on its structural properties, NA1-115–7 appears to be a molecule that respects Lipinski's rule of five for orally bioavailable drugs (Log P: 3.50, MW: 396.48, only 1 hydrogen bond donor and 5 hydrogen bond acceptors) (Lipinski et al., 1997). At pH = 7.4, NA1-115–7 was not ionized and its thermodynamic solubility was 357.5 ± 9.8 μM, i.e., 141.7 ± 3.9 μg/mL, as determined by the shake-flask method. According to the results of the PAMPA GIT test, NA1-115–7 has a relatively low permeability value across the gastrointestinal barrier at all pHs tested (Table 2). After 4 h of incubation at pH = 5, variable results with a high standard deviation were obtained, probably due to the instability of the compound under acidic conditions.

We studied the stability of NA1-115–7 in digestive media. NA1-115–7, initially dissolved at 10.1 mM (4.0 mg/mL) in DMSO, was added to various biomimetic media (1:100 dilution) before immediate quantification of the solubilized drug. The amount of solubilized NA1-115–7 appeared to be higher in the intestinal media (96.5 ± 0.6 μM in the simulated fasted state - FaSSIF, and 94.7 ± 0.5 μM in the fed state - FeSSIF) than in the simulated gastric fluid (SGF, 78.3 ± 0.3 μM). Under these conditions, the equilibrium solubility of NA1-115–7 was attained from the beginning of the experiment in both intestinal media, not being significantly ($p > 0.05$) affected by the presence of bile salts and phospholipids (Fig. 1).

Approximately 16 % of the NA1-115–7 was lost after 1 h in both simulated intestinal media before a steady state was reached. In the biomimetic acidic environment of the stomach, the fraction of the solubilized drug gradually decreased over time and after 3 h, only about 14 % of the NA1-115–7 was recovered, i.e., 10.7 ± 0.1 μM, which is significantly different than at the beginning of the experiment ($p < 0.05$) (Fig. 1). Such results cannot be explained by a difference in the ionized state of NA1-115–7 as, based on its pKa values (Table 2), the molecule is un-ionized in the various media. The instability in SGF was related to the degradation of NA1-115–7 over time, as shown by the appearance of a second peak on the HPLC chromatogram at $t_R = 2.24$, which increased over time and became predominant 3 h after the start of the experiment (results not shown). Indeed, we have previously shown that a close analogue of NA1-115–7 was sensitive to acidic conditions and spontaneously rearranged into a lactone (Fig. 2) due to the presence of the 6α-OH (Fomekong Fotsop et al., 2008).

Table 2
Properties of NA1-115–7.

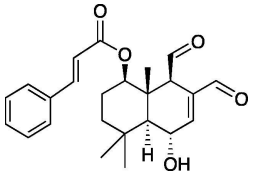

Molecular weight (g/mol)	396.48
p*Ka*	> 12
Log*P*	3.50
Melting point (°C)	157.0 ± 1.0
Thermodynamic solubility at pH 7.4 (μM)	357.5 ± 9.8
PAMPA gastrointestinal tract permeability assay at pH 5: Pe (nm/s)	49.9 ± 72.6
PAMPA gastrointestinal tract permeability assay at pH 6: Pe (nm/s)	26.5 ± 5.1
PAMPA gastrointestinal tract permeability assay at pH 7.4: Pe (nm/s)	20.3 ± 2.5

pKa and LogP (Consensus method) were calculated using ChemAxon software.

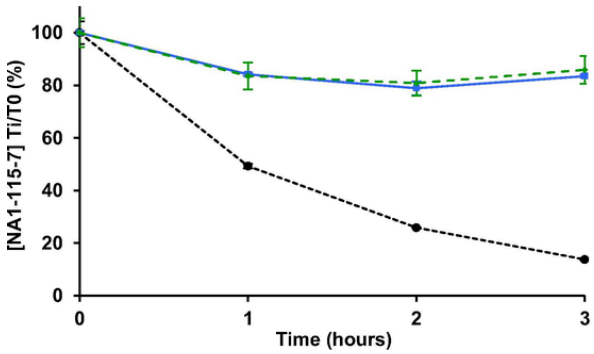

Fig. 1. Kinetic solubility of NA1-115–7 in SGF (in black), FaSSIF (in blue), and FeSSIF (in green) media at 37 °C (n = 3, data are shown as the mean ± SD). (For interpretation of the references to colour in this figure legend, the reader is referred to the web version of this article.)

As the usual transit time in the stomach is between 15 min and 3 h (Javadzadeh and Hamedeyazdan, 2012), it is crucial to find solutions that allow the stabilization of NA1-115–7 under acidic conditions to enable preclinical development, especially since oral administration is envisaged during early animal experiments.

3.2. NA-NE formulation and characterization

A nanoemulsion formulation has been recently developed according to a specific mixture design and after a careful selection of excipients on the basis of their safety profile and proven on human whole blood using a miniaturized process (Séguy et al., 2020). Given the interest of this approach in solubilizing and stabilizing chemotherapeutic molecules (Ceramella et al., 2021), we decided to apply this formulation strategy to NA1-115–7. NA-NEs appear to have been successfully formulated by a spontaneous self-emulsification process using a drug loading rate of 1 to 4.9 wt% (Table 3) in light of the critical product attributes of paricle size, zeta potential, and drug content that were achieved.

Monodisperse nanoemulsions could be formulated from a low drug payload of 10 mM to a high drug payload of 24.0 ± 2.0 mM (i.e., 9.5 ± 0.8 mg/mL). At these concentrations, the drug added to the anhydrous mixture during the formulation process appeared to be completely dissolved. After the addition of the aqueous phase, a homogeneous colloidal suspension was observed. Remarkably, these nanoemulsions did not undergo Ostwald ripening, as their granulometric properties remained highly stable for more than three weeks of storage at 4 °C (Fig. 3a). The formulation resulted in a > 60-fold increase in the apparent solubility of NA1-115–7 relative to the thermodynamic solubility of NA1-115–7 at pH 7.4. However, over time, some NA1-115–7 molecules precipitated before reaching thermodynamic equilibrium (Fig. 3b). Indeed, the drug payload did not change significantly after 7 days ($p > 0.05$).

We then evaluated the ability of NEs to protect NA1-115–7 in the acidic gastric environment by adding NA-NEs, with an initial concentration of 10.2 mM (4.0 mg/mL), to a simulated gastric fluid solution. After a 1:100 dilution, the kinetic solubility of the drug was assessed at 37 °C and compared to that of free NA1-115–7 (Fig. 4).

NA1-115–7 appeared to be fully available once the NA-NE formulation was diluted in SGF (NA1-115–7 concentration of 113.0 ± 1.1 µM at the start of the experiment, Fig. 4a). NEs appear to be an attractive approach for carrying this drug and allowing its oral administration while controlling the dose, as this concentration is considerably higher than that of the free form of NA1-115–7 (78.3 ± 0.3 µM at t_0). Over time, the droplets apparently partially reorganized and released some NA1-115–7 into the biomimetic gastric medium, as indicated by the increase in PDI and average diameter of the NEs (Fig. 4b). Nevertheless, the NEs appeared to significantly stabilize the NA1-115–7 ($p < 0.0001$), as approximately 56 % of the molecule was recovered in the medium after three hours. This is equivalent to a final concentration of 63.4 ± 0.7 µM, i.e., six times higher than that for the non-encapsulated molecule (10.7 ± 0.1 µM,).

3.3. Biological evaluation of the nanoemulsions

3.3.1. In vitro cytotoxicity of NEs on BL2 cells

We evaluated the cytotoxicity of the blank NEs, after dilution in RPMI 1640 medium by a cell proliferation MTT assay on the MCL-1 and BCL-xL-dependent BL2 (Burkitt lymphoma) cell line. This cell line showed good sensitivity to NA1-115–7, as, after treatment for 24 h, a lethal concentration 50 (LC_{50}) of 3.6 µM was determined (Daressy et al., 2021).

We then compared the cytotoxicity of the blank NEs to that of each excipient used in similar proportions to the corresponding diluted NEs (Fig. 5). After 24 h of exposure of the cells to the formulations, neither Labrafac® WL 1349, a medium chain triglyceride, nor Transcutol® HP, a high-purity solvent and solubilizer, affected the growth of BL2 cells at any concentration. Cell survival was only slightly decreased (< 20 %) at a 1:2,000 dilution of the blank NEs (i.e., a corresponding concentration of 120.6 µg/mL in anhydrous excipients), with an estimated LC_{50} of 236 µg/mL. The observed toxicity could be attributable to Kolliphor® HS 15, as its LC_{50} of 132 µg/mL is consistent with the proportion of this non-ionic surfactant used in the formulation (55 %, w/w). Therefore, exposure of cells to levels below this concentration of blank NEs, and ideally after a 1:4,000 dilution to eliminate any cytotoxicity, should be performed before use on BL2 cells. Given the NA1-115–7 payloads of 10.2 and 24.0 mM (4 and 9.5 mg/mL, respectively), it should be possible to explore the effects of NA1-115–7 on BL2 cells with concentrations up to 2.5 and 6 µM, i.e., beyond the LC_{50} of the drug.

3.3.2. In-vitro efficacy of NA-NEs

In our previous study, we determined that the LC_{50} of NA1-115–7 was equal to 3.1 µM and 12 µM in the BL2 and Remb1 cell lines, respectively (Daressy et al., 2022). The mechanism of NA1-115–7 induced cell death was explored by incubating cell lines for 24 h without or with 4 µM NA1-115–7 (Daressy et al., 2022).To enable a comparison of effect, in the present study, BL2 and Remb1 cells were treated with either free NA1-115–7 (2 and 4 µM), blank NEs (equivalent to a 2 µM treat-

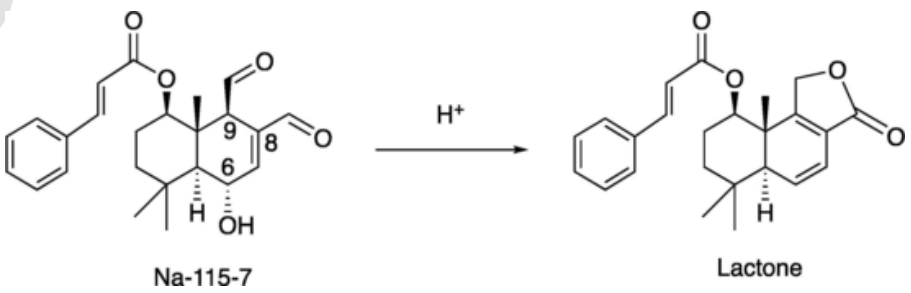

Fig. 2. Rearrangement of NA1-115–7 in acidic media.

Table 3
Physicochemical properties of blank (i.e., unloaded) and NA-NEs (n = 22, data are presented as the mean ± SD).

	Z-average diameter (nm)	PDI	ζpotential (mV)	Encapsulation efficiency (%)	NA1-115–7 payload
Blank NEs	50.6 ± 2.6	0.176 ± 0.014	– 4.7 ± 3.1	–	–
NA-NEs	41.9 ± 2.2	0.131 ± 0.016	– 5.8 ± 3.4	98.9 ± 5.9	9.5 ± 0.8 mg/mL 24.0 ± 2.0 mM

NA1-115–7-loaded droplets appeared to be homogeneous in size (polydispersity index value < 0.2), with a mean diameter of 41.9 ± 0.4 nm (Table 3). NA1-115–7 encapsulation slightly but significantly decreased the hydrodynamic diameter and PDI of the nanodroplets ($p < 0.001$), without modifying the zeta potential, which remained neutral for both blank-NEs and NA-NEs. Given the high encapsulation efficiency of NA1-115–7 in NEs, a drug payload of 24.0 ± 2.0 mM (i.e., 9.5 ± 0.8 mg/mL) was obtained.

ment), or NA-NEs (2 μM) for 24 h. Apoptosis was then quantified after annexin V / PI labeling (Fig. 6).

Importantly, blank-NEs alone, at a concentration equivalent to the 2 μM treatment, were found to be nontoxic and, thus, did not induce apoptosis in the BL2 or Remb1 cell lines. In the BL2 cell line, 4 μM free NA1-115–7 induced 86 ± 3 % apoptosis, whereas a concentration of 2 μM induced 47 ± 5 % apoptosis (Fig. 6a). Treatment of BL2 cells with 2 μM NA-NEs was sufficient to induce 88 ± 3.5 % apoptosis. The treatment doses could therefore be reduced from 4 μM to 2 μM while maintaining substantial induction of apoptosis in this cell line. By contrast, treatment of BCL-xL-dependent Remb1 cells with 2 μM NA-NEs only weakly induced apoptosis (19.5 ± 3 % apoptotic cells). A similar percentage of apoptotic cells was measured after treatment with free NA1-115–7: 16.5 ± 3 % for 2 μM and 22 ± 2.5 % for 4 μM (Fig. 6b). These results are coherent with the LC_{50} of 12.2 μM previously determined for free NA1-115–7 on Remb1 cells and confirm the MCL-1 specificity of the drug, either free or encapsulated into NEs.

3.3.3. *In vitro toxicity on healthy cells*

It was important to confirm that the observed increase in cytotoxic activity was not associated with higher toxicity in healthy cells. Thus, NA-NEs were tested on PBMCs isolated from healthy donors and apoptosis was quantified after annexin V/PI labelling (Fig. 7). First, blank-NEs at a concentration equivalent to 2 μM treatment did not induce apoptosis of PBMCs, confirming the safety of NEs. Compared to the results obtained with 0.5 μM S63845 (61 ± 4 %), a known MCL-1 inhibitor, low apoptosis of 16 ± 2 % was observed after treatment with 2 μM NA-NEs and 21.5 ± 2 % after treatment with 4 μM free NA1-115–7.

4. Discussion

Since 2016, six MCL-1 inhibitors (S64315/MIK665, AZD-5991, AMG-176, AMG-397, ABBV-467, and PRT1419) have been evaluated in clinical trials for the treatment of multiple myeloma, acute myeloid leukemia, and various types of lymphoma. However, only two molecules are still currently in clinical development. Trials of AMG-176 (NCT02675452 and NCT03797261) were halted due to cardiac toxicity, AZD-5991 (NCT03218683) for potential safety reasons, and those of AMG-397 and ABBV-467 (NCT03465540 and NCT04178902) were prematurely suspended for strategic reasons. PRT1419 is currently under evaluation in a Phase I clinical trial in patients with relapsed/refractory hematological malignancies (NCT04543305) and trials of S64315 in combination with MIK665 (NCT04702425 and NCT03672695) are still ongoing. Importantly, these inhibitors bind to MCL-1 with nanomolar

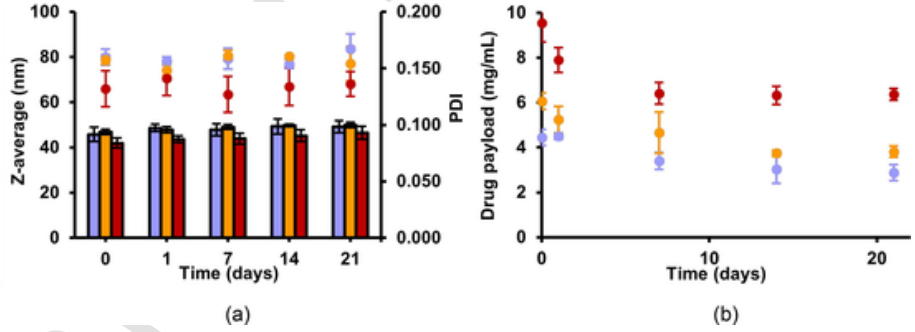

Fig. 3. Evolution over time of **a.** the granulometric properties (hydrodynamic diameter shown as the Z-average (bars) and subsequent PDI (points)) of NA-NEs stored at 4 °C formulated with increasing loading rates of NA1-115–7 (in blue for 4 mg/mL, orange for 6 mg/mL, and red for 9 mg/mL) and **b.** their resulting drug payloads ($n \geq 3$, data are shown as the mean ± SD). (For interpretation of the references to colour in this figure legend, the reader is referred to the web version of this article.)

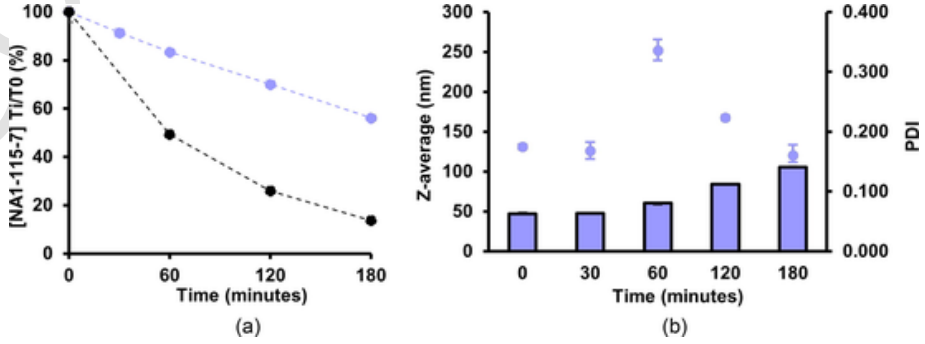

Fig. 4. A. Comparison over time of solubilized NA1-115–7 in SGF at 37 °C in a DMSO solution (in black) with the NA-NE formulation under the same conditions (in blue). **b.** Concomitant evolution of the granulometric properties (hydrodynamic diameter shown as the Z-average (bars) and subsequent PDI (points)) of the NA-NEs in SGF at 37 °C (n = 3). (For interpretation of the references to colour in this figure legend, the reader is referred to the web version of this article.)

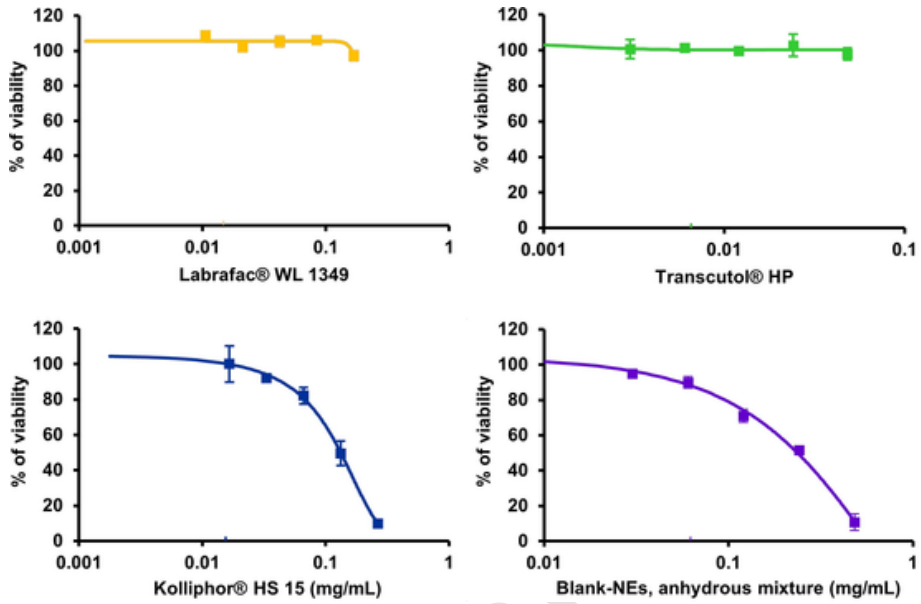

Fig. 5. Viability of BL2 cells after 24 h of exposure to various concentrations of the aqueous suspension of blank-NEs or the respective proportions of each excipient used in NEs (n = 3, data are expressed as the mean ± SD). The results obtained for BL2 cells with vehicle alone are considered to correspond to 100 % survival.

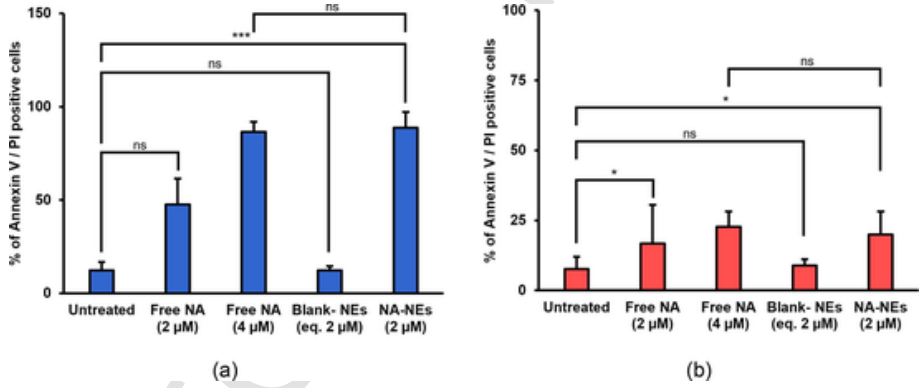

Fig. 6. Induction of apoptosis was measured on the BL2 (a) or Remb1 (b) cell lines after 24 h of treatment with 2 and 4 µM free NA1-115–7, blank-NEs at a concentration equivalent to a treatment of 2 µM (eq. 2 µM), or 2 µM NA-NEs by annexin V/PI labelling analyzed by cytometry. The values presented (mean ± SD) are from at least five independent experiments (*$p < 0.05$, ***$p < 0.001$, ns: nonsignificant).

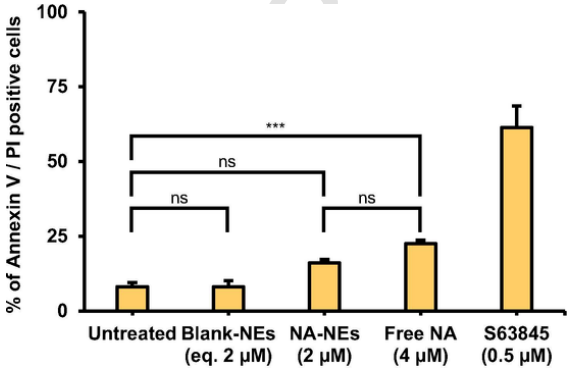

Fig. 7. Induction of apoptosis was measured on PBMCs after 24 h of treatment with blank-NEs at a concentration equivalent to a treatment of 2 µM (Blank-NEs (eq.2 µM)), 2 µM NA-NEs, 4 µM free NA1-115–7, or 0.5 µM S63845 by annexin V/PI labeling analyzed by cytometry. The values presented (mean ± SD) are from at least four independent experiments (***$p < 0.001$, ns: nonsignificant).

affinity (Caenepeel et al., 2020; Szlavik et al., 2020). However, the safety of MCL-1 inhibitors may be an important issue in their clinical development, as knocking out MCL-1 may lead to cardiotoxicity problems (Daressy et al., 2022). This implies that there is still a need for safer alternative molecules.

NA1-115–7, a natural product isolated from *Zygogynum ancheri*, recently appeared as a promising new selective inhibitor of MCL-1 (Daressy et al., 2021). To establish the drugability profile of this MCL-1 inhibitor, certain relevant physicochemical properties of NA1-115–7 were first investigated (Table 2). With a solubility of 157.0 µM at pH 7.4, NA1-115–7 appeared to be poorly soluble in water. This has also been shown to be true for other MCL-1 inhibitors. For example, an aqueous solubility of 9.4 µM has been reported for pyridoclax (De Pascale et al., 2020). The experimentally determined solubilities of the MCL-1 inhibitors currently in clinical trials are not published, which prevents direct comparison with NA1-115–7. However, two, i.e., S64315 and AZD-5991, are formulated in 20 % or 30 % 2-hydroxypropyl-beta-cyclodextrin (HPβCD), respectively, which is an FDA-approved excipient to increase the aqueous solubility of many hydrophobic compounds (Davis and Brewster, 2004; Gidwani and Vyas, 2015). Using a PAMPA assay, a high-throughput technique commonly used in drug discovery to predict passive permeation through biological membranes, we evaluated the ability of NA1-115–7 to cross the gas-

trointestinal tract. NA1-115–7 exhibited poor permeability (Pe = 20.6 to 49.9 nm/s for pH 7.4 to pH 5). A threshold value of *P*e > 100 nm/s is the generally accepted threshold value to consider that permeation is not a limiting factor for oral bioavailability, which would not be the case for NA1-115–7 (Veber et al., 2002). The PAMPA assay may provide valuable information about the permeability of single molecules, and in certain cases, of more complex substrates, such as extracts and formulations (Piazzini et al., 2017). PAMPA and Caco–2 cells have similar predictivity for passive oral absorption (Avdeef et al., 2007). Thus, the PAMPA method is well suited for the early stages of drug discovery, although it does not provide any information on absorption involving transporter-mediated processes, such as active uptake or efflux (Kansy et al., 1998; Avdeef et al., 2007). In further preclinical steps, it would be informative to study the *ex vivo* mucosal permeability of the NA1-115–7 formulation to obtain additional predictive permeability data (Hosny et al., 2021, 2019). Here, stability assays in biorelevant media also showed that NA1-115–7 is unstable in an acidic environment. It is, thus, likely that NA-115–7 spontaneously rearranges to a lactone in the biomimetic acidic environment of the stomach (Fig. 2). Based on our previous structure–activity relationship (SAR) studies on this chemical series (Daressy et al., 2021), this lactone is inactive on the MCL-1 protein.

To overcome these issues, which could limit the clinical development of NA1-115–7, we resorted to nanomedicines, as already done for other natural anticancer compounds (Gong et al., 2017; Ma et al., 2019). For example, nanomedicine strategies have been successfully applied to baicalin and its aglycone, baicalein, the major bioactive flavones derived from *Scutellaria baicalensis* (Gong et al., 2017). Drug-delivery nanosystems can address the bioavailability issues related to these compounds by improving their oral bioavailability, enhancing their anti-cancer activity, and reducing their side-effects.

Previously, we sought to develop a versatile drug-delivery system that would be particularly useful for poorly soluble drugs. The resulting nanoemulsions were formulated by the spontaneous nanoemulsification method using three excipients: Labrafac® WL 1349, composed of medium-chain triglycerides, Kolliphor® HS15, a nonionic surfactant, and Transcutol® HP, a high-purity solvent and solubilizer. This formulation was developed by carefully designed mixture experiments using a ternary oil/surfactant/cosurfactant phase diagram to determine the self-nanoemulsifying region with appropriate properties (Séguy et al., 2020). These nanoemulsions have been applied to several drugs without modification of the composition or formulation process (Ceramella et al., 2021; Séguy et al., 2021). NA1-115–7-loaded NEs were also successfully formulated in the present study. Its encapsulation weakly decreased the size and PDI of the nanodroplets without modifying the zeta potential, which remained neutral (Table 3). The neutral zeta-potential value is consistent with the nature of the excipients (medium-chain triglyceride, diethylene glycol monoethyl ether, and macrogol 15 hydroxystearate), and the un-ionized state of the drug at pH 7.4. The encapsulation of NA1–115–7 increased its solubility by > 60-fold, as a maximal payload of approximately 9.5 mg/mL was obtained (Fig. 3). Thus, this formulation appears to be relatively close to a supersaturated lipid-based formulation (sLBF). Indeed, NA1-115–7 appears to become spontaneously oversaturated in the droplets of the nanoemulsions after the addition of excess drug to the excipients. As with other sLBFs, precipitation eventually occurs, depending on the drug properties, lipid vehicle, supersaturation ratio, and storage conditions, as dictated by the thermodynamic solubility of the drug in the vehicle. Such behavior has recently been reported for venetoclax in sLBFs. This selective B-cell lymphoma 2 (Bcl-2) inhibitor, approved in 2016 for the treatment of leukemia, appeared to violate the classical Lipinski's rule of five. As it required a biologically driven formulation approach to overcome its solubility and/or permeability issues, it was formulated with defined oils and monoglycerides. The resulting sLBF appeared to be a good strategy to promote and maintain supersaturation of the drug and *in fine* to achieve higher oral bioavailability of the drug (Koehl et al., 2020).

Based on our results, the nanoemulsions did not undergo Ostwald ripening, as their granulometric properties remained highly stable for more than three weeks of storage at 4 °C and even at room temperature (results not shown).

We then evaluated the ability of NEs to protect NA1-115–7 in the acidic gastric environment by adding NA-NEs to a simulated gastric fluid solution. Encapsulation of NA1-115–7 into NEs made it possible to obtain higher concentrations of the drug than in its free form at t_0. Although the NA-NEs partially reorganized and released some NA1-115–7 molecules into the biomimetic gastric medium (Fig. 3b), the concentration of the molecule was sixfold higher than that of the non-encapsulated molecule after three hours (Fig. 1). It is known that the residence time in the stomach varies due to many parameters (age, species, fasting or feeding state, the volume of food intake, etc.). Moreover, given that gastric emptying for liquid administration is rapid and most of the contents are evacuated within the first hour, the stabilization of NA1-115–7 through the formulation of NEs appears to be a promising means to further consider preclinical studies of NA1-115–7 after oral administration.

To better anticipate future *in vivo* tests, the development of in vitro experiments capable of providing information on cytotoxicity in preclinical studies is necessary (Fattal and Hillaireau, 2020). Our proposed NEs for NA1-115–7 encapsulation are formulated using an organic solvent-free method. Indeed, the use of organic solvents can cause safety issues and dose limitations due to their toxicity. The present nanoemulsions were developed from anhydrous mixtures composed of excipients already described in the European Pharmacopeia (World Health Organization, 2018) and already proven to be hemocompatible on human whole blood (Séguy et al., 2020).

Among the three excipients that comprise the nanoemulsions, only Kolliphor® HS15 showed toxicity on the BL2 cell line (Fig. 5). Nevertheless, due to its unique solubilization characteristics and safety profile, this solubilizer, with inherent amphiphilicity stemming, has been widely used in parenteral and oral formulations for several decades (Ruchatz and Schuch, 1998). Kolliphor® HS 15 is included, for example, in the formulations of orodispersible tablets of phloroglucinol, administered orally, travoprost eye drops, administered ophthalmically, or rolapitant injection, administered intravenously. As for all surfactants, it can induce adverse effects at high concentrations. This is true, for example, for Kolliphor® EL (formerly known as Cremophor® EL), a non-ionic surfactant included in injectable paclitaxel solutions that can induce non-allergic hypersensitivity reactions (Gelderblom et al., 2001). According to the toxicity studies carried out by the manufacturer, repeated administration of Kolliphor® HS 15 to dogs can also cause pseudo-allergic reactions (no observed-adverse-effect level (NOAEL) = 25 mg/kg/d), but these were completely reversible and less serious than those after administration of Kolliphor® EL under the same conditions (lowest-observed-adverse-effect level (LOAEL) = 5 mg/kg/d)). When used alone, Kolliphor® HS15 is known to form 13–14 nm sized micelles in an aqueous medium above its critical micelle concentration (CMC) (0.06–0.1 mM, corresponding to approximately 55–95 μg/mL), regardless of the nature of the aqueous buffer. On epithelial cells, this surfactant has been shown to exert significant toxicity at concentrations above its CMC (Shubber et al., 2015). Surfactant monomers, eventually provided by micelles, could potentially become incorporated into the cell membrane. By inducing a subsequent disorder in the phospholipid bilayer following its insertion, Kolliphor® HS15 could induce an increase in membrane permeability, and therefore toxicity.

The high encapsulation efficiency of NA1-115–7 into NEs of up to 22.7 mM and the non-apparent toxicity of NEs when the payloads are between 10.2 and 22.7 mM show promise for its biological evaluation. Thus, to further investigate the ability of NEs to transport NA1-115–7,

we explored its efficacy in vitro by quantifying apoptosis in two hematological cell lines: BL2, a Burkitt lymphoma cell line, dependent on MCL-1 and BCL-xL, and Remb1, a lymphoblastoid cell line (EBV-transformed normal B lymphocytes), dependent on BCL-xL and useful for evaluating resistance to apoptosis (Daressy et al., 2021).

Efficacy results obtained on the MCL-1-dependent BL2 cell line suggest that NA-NEs were more effective than free NA1-115–7 in inducing apoptosis; the treatment doses could therefore be reduced from 4 μM to 2 μM while maintaining a marked induction of apoptosis in this cell line (Fig. 6a). By contrast, treatment of BCL-xL-dependent Remb1 cells with 2 μM NA-NEs was only weakly associated with apoptosis. In previous studies, we showed that free NA1-115–7 is a new BH3-mimetic that is selective for MCL-1 and capable of inducing the apoptosis of hematopoietic tumoral cells via BAK and BAX activation, followed by the release of apoptogenic factors (SMAC and cytochrome *c*) from the mitochondria (Daressy et al., 2021, 2022).

By forming a covalent bond with a lysine residue in the BH3-groove of MCL-1, NA1-115–7 is the first MCL-1 inhibitor that acts as a "suicide molecule", as it remains in the dying cells. This property may limit its use in tumoral cells expressing high levels of MCL-1, which would thus require high doses of NA1-115–7. By contrast, it ensures its efficacy in MCL-1-dependent cells, even if they do not overexpress MCL-1. For example, this is true for myeloma cells that do not harbor an amplification of the 1q arm (approximately 60 % of de novo and 30 % of relapsed patients) but are still sensitive to MCL-1 inhibitors (Seiller et al., 2020). Thus, NEs offer an advantage by preserving the specificity of the compound and increasing its efficacy. A similar improvement in compound efficacy has already been observed for another NE formulation applied to the MCL-1 inhibitor, pyridoclax, evaluated on the IGROV1-R10 ovarian cancer cell line (Groo et al., 2020). In this study, it was established that encapsulation of pyridoclax in NEs provided a 2.5-fold increase in the cytotoxic activity of the MCL-1 inhibitor relative to that of free pyridoclax (Groo et al., 2020). This activity was illustrated by a strong increase in caspase 3/7 activation from 10 μM pyridoclax-loaded NEs. The interaction between NEs and a membrane component, such as phospholipids, or the extracellular matrix of cells can promote the entry of nanocarriers into the cell by endocytosis (Shubber et al., 2015). As already mentioned, Kolliphor® HS15 could induce a subsequent disorder in the cellular phospholipid bilayer following its insertion, but an increase in the rate of endocytosis in the presence of this surfactant at permeability-enhancing concentrations has also been reported (Shubber et al., 2015). Here, the presence of Kolliphor® HS15 could partially explain the enhanced cellular uptake by endocytosis.

Before considering *in vivo* preclinical studies, it is necessary to evaluate the safety of NE-NAs on healthy cells. Our results show that, as for free NA1-115–7, NA-NEs are not associated with toxicity in healthy PBMCs (Fig. 7). However, many MCL-1 inhibitors have encountered safety problems in clinical trials, notably due to cardiac adverse events. Through MTT and hERG inhibition assays, NA1-115–7 has not been shown to be cardiotoxic (Daressy et al., 2022). Given that MCL-1 inhibitors can be associated with cardiac toxicity via on-target/off-tumor effects due to the involvement of MCL-1 in mitochondrial cell function, these results appear to be meaningful (Rasmussen et al., 2020; Wang et al., 2013). For example, AZD-5991 combined with venetoclax is currently on a clinical hold due to an asymptomatic elevation in cardiac biomarkers (NCT03218683). These results allow us to consider NA-NEs as a solution for the evaluation of the cytotoxic activity of this compound *in vivo*. Thus, the NA-NE approach appears to be effective in stabilizing NA1-115–7 under acidic conditions, hence allowing its oral administration while also providing a twofold reduction in its therapeutic concentration, leading to fewer potential cytotoxic effects. No toxicity to erythrocytes, PBMCs, platelets, or cardiomyocytes, nor cardiotoxicity by hERG testing, have been observed (Daressy et al., 2022). In contrast to previous clinical trials on MCL-1 inhibitors, we propose a galenic strategy, which allows a reduction in the dose used, therefore reducing the cost associated with the quantity of the drug and the risk of adverse effects. Indeed, nanodrug-delivery systems are known to achieve a lower drug dose by consistently delivering the drug to tumor sites, thus reducing side effects (Gong et al., 2017). Among nanocarriers, nanoemulsions are currently being envisaged as an effective drug-delivery approach for cancer therapeutics because of their advantages (biodegradability, biocompatibility, nanometric size range with a large surface area, non-immunogenicity, ease of formulation, and thermodynamic stability). However, there are challenges associated with the clinical translation of nanoformulations. For further development, material safety (for the health and the environment), scale-up issues, and quality control problems, as well as legal, consumer, and economic factors, will need to be addressed to maximally exploit the NE perspective in the clinical setting (Alshahrani, 2022; Ozogul et al., 2022).

5. Conclusion

In previous studies, we have shown free NA1-115–7 to be a new BH3-mimetic selective for MCL-1 capable of inducing the apoptosis of hematopoietic tumoral cells. At doses toxic to tumoral cells, NA1-115–7 did not induce apoptosis of normal blood cells (PBMCs, platelets, erythrocytes) or cardiomyocytes and is thus a potential new tool for the treatment of cancer cells. However, certain drugability parameters, i.e., its hydrophobic character, its limited passive gastro-intestinal permeability, and its instability in acidic conditions, could hamper its preclinical value and its further clinical development. Here, we were able to overcome the challenge of limited solubility and stability through the use of nanoemulsions. Considering that the formulation itself may not be exempt from having biological effects, we characterized the cytotoxicity profile of the nanoemulsions to define the optimal conditions for use in *in vitro* evaluations. Our biocompatible formulation preserved the specificity of NA1-115–7 as an MCL-1 inhibitor, inducing the death of lymphoproliferation cells by activation of the apoptotic mitochondrial pathway. Indeed, the nanoemulsions even increased the efficiency of the compound on hematological cells, while showing no toxicity in healthy PBMCs, offering a considerable advantage in the perspective of their *in vivo* evaluation. Overall, considering the various application possibilities of the developed nanoemulsions, they can offer a versatile formulation solution to overcome solubility and stability issues of drugs and promote the development of new therapeutic approaches.

Furthermore, NA1-115–7 harbors a specific feature, as it is the first MCL-1 inhibitor to act as a "suicide molecule". This property may limit its use in tumoral cells expressing high levels of MCL-1 and thus requiring high doses of NA1-115–7, which are modulable with the use of the nanoemulsions. By contrast, it ensures its efficacy against MCL-1-dependent cells, such as myeloma cells, and NA-NEs could represent a novel potential strategy for cancer treatment. Xenografts of such tumoral cells would therefore constitute a useful model for the *in vivo* evaluation of the effects of NA-NEs. In a further work, pharmacokinetics studies should also be performed to determine the biodistribution of the encapsulated drug to finally establish the potential of the NEs, not only to improve the stability of NA1-115–7 but also its bioavailability.

Uncited reference

International Conference on Harmonisation (ICH) of Technical Requirements for Registration of Pharmaceuticals for Human Use (2005).

CRediT authorship contribution statement

Line Séguy : Formal analysis, Investigation, Writing – original draft. **Florian Daressy :** Formal analysis, Investigation. **Sophia Lahlil :** Investigation. **Sophie Corvaisier :** Formal analysis, Investigation. **Vincent Dumontet :** Investiga-

tion. **Marc Litaudon :** Investigation. **Cécile Appel :** Investigation. **Fanny Roussi :** Conceptualization. **Joëlle Wiels :** Conceptualization. **Aude Robert :** Formal analysis, Conceptualization, Methodology. **Anne-Claire Groo :** Formal analysis, Investigation, Methodology, Writing – original draft, Funding acquisition. **Aurélie Malzert-Fréon :** Conceptualization, Methodology, Writing – review & editing.

Declaration of Competing Interest

The authors declare that they have no known competing financial interests or personal relationships that could have appeared to influence the work reported in this paper.

Data availability

No data was used for the research described in the article.

Acknowledgements

This work was financially supported by the "Ligue contre le cancer" (Calvados committee, Nemibly project). L. Seguy was recipient of a doctoral fellowship from the Caen teaching hospital. This work was financially supported by the I2C and the Chimie Balard CIRIMAT Carnot Institutes, the Region Normandie and the European Union via the European Regional Development Fund (FEDER).

References

Allouche, N., Apel, C., Martin, M.-T., Dumontet, V., Guéritte, F., Litaudon, M., 2009. Cytotoxic sesquiterpenoids from Winteraceae of Caledonian rainforest. Phytochemistry 70, 546–553. https://doi.org/10.1016/j.phytochem.2009.01.012.

Alshahrani, S.M., 2022. A judicious review on the applications of chemotherapeutic loaded nanoemulsions in cancer management. J. Drug Delivery Sci. Technol. 68, 103085. https://doi.org/10.1016/j.jddst.2021.103085.

Anjani, Q.K., Sabri, A.H.B., Donnelly, R.F., 2022. Development and validation of simple and sensitive HPLC-UV method for ethambutol hydrochloride detection following transdermal application. Anal. Methods 14, 125–134. https://doi.org/10.1039/D1AY01414E.

Avdeef, A., Bendels, S., Di, L.i., Faller, B., Kansy, M., Sugano, K., Yamauchi, Y., 2007. PAMPA—critical factors for better predictions of absorption. JPharmSci 96 (11), 2893–2909.

Bhagwat, N., Grego, A., Gowen-MacDonald, W., Wang, M., Cowart, M., Wu, X., Zhuo, J., Combs, A., Ruggeri, B., Scherle, P., Vaddi, K., 2021. Abstract 983: Preclinical characterization of PRT1419, a potent, selective and orally available inhibitor of MCL1. Cancer Research 81, 983. 10.1158/1538-7445.AM2021-983.

Caenepeel, S., Brown, S.P., Belmontes, B., Moody, G., Keegan, K.S., Chui, D., Whittington, D.A., Huang, X., Poppe, L., Cheng, A.C., Cardozo, M., Houze, J., Li, Y., Lucas, B., Paras, N.A., Wang, X., Taygerly, J.P., Vimolratana, M., Zancanella, M., Zhu, L., Cajulis, E., Osgood, T., Sun, J., Damon, L., Egan, R.K., Greninger, P., McClanaghan, J.D., Gong, J., Moujalled, D., Pomilio, G., Beltran, P., Benes, C.H., Roberts, A.W., Huang, D.C., Wei, A., Canon, J., Coxon, A., Hughes, P.E., 2018. AMG 176, a Selective MCL1 Inhibitor, Is Effective in Hematologic Cancer Models Alone and in Combination with Established Therapies. Cancer Discov 8, 1582–1597. 10.1158/2159-8290.CD-18-0387.

Caenepeel, S., Karen, R., Belmontes, B., Verlinsky, A., Tan, H., Yang, Y., Chen, X., Li, K., Allen, J., Wahlstrom, J., Canon, J., Coxon, A., Hughes, P., 2020. Abstract 6218: Discovery and preclinical evaluation of AMG 397, a potent, selective and orally bioavailable MCL1 inhibitor. Cancer Research 80, 6218. 10.1158/1538-7445.AM2020-6218.

Campbell, K.J., Bath, M.L., Turner, M.L., Vandenberg, C.J., Bouillet, P., Metcalf, D., Scott, C.L., Cory, S., 2010. Elevated Mcl-1 perturbs lymphopoiesis, promotes transformation of hematopoietic stem/progenitor cells, and enhances drug resistance. Blood 116, 3197–3207. https://doi.org/10.1182/blood-2010-04-281071.

Ceramella, J., Groo, A.-C., Iacopetta, D., Séguy, L., Mariconda, A., Puoci, F., Saturnino, C., Leroy, F., Since, M., Longo, P., Malzert-Fréon, A., Sinicropi, M.S., 2021. A winning strategy to improve the anticancer properties of Cisplatin and Quercetin based on the nanoemulsions formulation. J. Drug Delivery Sci. Technol. 66, 102907. https://doi.org/10.1016/j.jddst.2021.102907.

Couvreur, P., Vauthier, C., 2006. Nanotechnology: intelligent design to treat complex disease. Pharm Res 23, 1417–1450. https://doi.org/10.1007/s11095-006-0284-8.

Daressy, F., Malard, F., Seguy, L., Guérineau, V., Apel, C., Dumontet, V., Robert, A., Groo, A.-C., Litaudon, M., Bignon, J., Desrat, S., Malzert-Fréon, A., Wiels, J., Lescop, E., Roussi, F., 2021. Drimane Derivatives as the First Examples of Covalent BH3 Mimetics that Target MCL-1. ChemMedChem 16, 1789–1798. https://doi.org/10.1002/cmdc.202100011.

Daressy, F., Séguy, L., Favre, L., Corvaisier, S., Apel, C., Groo, A.-C., Litaudon, M., Dumontet, V., Malzert-Fréon, A., Desrat, S., Roussi, F., Robert, A., Wiels, J., 2022. NA1-115-7, from Zygogynum pancheri, is a new selective MCL-1 inhibitor inducing the apoptosis of hematological cancer cells but non-toxic to normal blood cells or cardiomyocytes. Biomed Pharmacother 154, 113546. https://doi.org/10.1016/j.biopha.2022.113546.

Davis, M.E., Brewster, M.E., 2004. Cyclodextrin-based pharmaceutics: past, present and future. Nat Rev Drug Discov 3, 1023–1035. https://doi.org/10.1038/nrd1576.

De Pascale, M., Iacopetta, D., Since, M., Corvaisier, S., Vie, V., Paboeuf, G., Hennequin, D., Perato, S., De Giorgi, M., Sinicropi, M.S., Sopkova-De Oliveira Santos, J., Voisin-Chiret, A.-S., Malzert-Freon, A., 2020. Synthesis of Pyridoclax Analogues: Insight into Their Druggability by Investigating Their Physicochemical Properties and Interactions with Membranes. ChemMedChem 15 (1), 136–154.

Delbridge, A.R.D., Strasser, A., 2015. The BCL-2 protein family, BH3-mimetics and cancer therapy. Cell Death Differ 22, 1071–1080. https://doi.org/10.1038/cdd.2015.50.

Fattal, E., Hillaireau, H., 2020. Nanotoxicologie et réglementation des nanomédicaments. Techniques de l'ingénieur.

Fomekong Fotsop, D., Roussi, F., Le Callonec, C., Bousserouel, H., Litaudon, M., Guéritte, F., 2008. Isolation and characterization of two new drimanes from Zygogynum baillonii and synthesis of analogues. Tetrahedron 64, 2192–2197. https://doi.org/10.1016/j.tet.2007.12.022.

García-Pinel, B., Porras-Alcalá, C., Ortega-Rodríguez, A., Sarabia, F., Prados, J., Melguizo, C., López-Romero, J.M., 2019. Lipid-Based Nanoparticles: Application and Recent Advances in Cancer Treatment. Nanomaterials 9, 638. https://doi.org/10.3390/nano9040638.

Gelderblom, H., Verweij, J., Nooter, K., Sparreboom, A., 2001. Cremophor EL: the drawbacks and advantages of vehicle selection for drug formulation. Eur. J. Cancer 37, 1590–1598. https://doi.org/10.1016/S0959-8049(01)00171-X.

Gidwani, B., Vyas, A., 2015. A Comprehensive Review on Cyclodextrin-Based Carriers for Delivery of Chemotherapeutic Cytotoxic Anticancer Drugs. Biomed Res Int 2015, 198268. 10.1155/2015/198268.

Glaser, S.P., Lee, E.F., Trounson, E., Bouillet, P., Wei, A., Fairlie, W.D., Izon, D.J., Zuber, J., Rappaport, A.R., Herold, M.J., Alexander, W.S., Lowe, S.W., Robb, L., Strasser, A., 2012. Anti-apoptotic Mcl-1 is essential for the development and sustained growth of acute myeloid leukemia. Genes Dev. 26, 120–125. https://doi.org/10.1101/gad.182980.111.

Gong, W.-Y., Zhao, Z.-X., Liu, B.-J., Lu, L.-W., Dong, J.-C., 2017. Exploring the chemopreventive properties and perspectives of baicalin and its aglycone baicalein in solid tumors. Eur J Med Chem 126, 844–852. https://doi.org/10.1016/j.ejmech.2016.11.058.

González, O., Blanco, M.E., Iriarte, G., Bartolomé, L., Maguregui, M.I., Alonso, R.M., 2014. Bioanalytical chromatographic method validation according to current regulations, with a special focus on the non-well defined parameters limit of quantification, robustness and matrix effect. Journal of Chromatography A, Method Validation 1353, 10–27. https://doi.org/10.1016/j.chroma.2014.03.077.

Groo, A.-C., De Pascale, M., Voisin-Chiret, A.-S., Corvaisier, S., Since, M., Malzert-Fréon, A., 2017. Comparison of 2 strategies to enhance pyridoclax solubility: Nanoemulsion delivery system versus salt synthesis. Eur. J. Pharm. Sci. 97, 218–226. https://doi.org/10.1016/j.ejps.2016.11.025.

Groo, A.C., Hedir, S., Since, M., Brotin, E., Weiswald, L.-B., Paysant, H., Nee, G., Coolzaet, M., Goux, D., Delépée, R., Freret, T., Poulain, L., Voisin-Chiret, A.S., Malzert-Fréon, A., 2020. Pyridoclax-loaded nanoemulsion for enhanced anticancer effect on ovarian cancer. Int. J. Pharm. 587, 119655. https://doi.org/10.1016/j.ijpharm.2020.119655.

Gué, E., Since, M., Ropars, S., Herbinet, R., Le Pluart, L., Malzert-Fréon, A., 2016. Evaluation of the versatile character of a nanoemulsion formulation. Int. J. Pharm. 498, 49–65. https://doi.org/10.1016/j.ijpharm.2015.12.010.

Hedir, S., De Giorgi, M., Fogha, J., De Pascale, M., Weiswald, L.-B., Brotin, E., Marekha, B., Denoyelle, C., Denis, C., Suzanne, P., Gautier, F., Juin, P., Ligat, L., Lopez, F., Carlier, L., Legay, R., Bureau, R., Rault, S., Poulain, L., Oliveira Santos, J.S., Voisin-Chiret, A.S., 2018. Structure-guided design of pyridoclax derivatives based on Noxa / Mcl-1 interaction mode. Eur. J. Med. Chem. 159, 357–380. https://doi.org/10.1016/j.ejmech.2018.10.003.

International Conference on Harmonisation (ICH) of Technical Requirements for Registration of Pharmaceuticals for Human Use, 2005. ICH Guideline, Validation of analytical prodecedures: text and methodology Q2(R1).

Hosny, Khaled M., Aldawsari, Hibah M., Bahmdan, Rahaf H, Sindi, Amal M., Kurakula, Mallesh, Alrobaian, Majed M., Aldryhim, Ahmed Y., Alkhalidi, Hala M, Bahmdan, Hiba Hisham, Khallaf, Rasha A., El Sisi, Amani M., 2019. Preparation, Optimization, and Evaluation of Hyaluronic Acid-Based Hydrogel Loaded with Miconazole Self-Nanoemulsion for the Treatment of Oral Thrush. AAPS PharmSciTech 20, 297. https://doi.org/s12249-019-1496-7.

Hosny, Khaled M., Sindi, Amal M., Alkhalidi, Hala M., Kurakula, Mallesh, Alruwaili, Nabil K, Alhakamy, Nabil A., Abualsunun, Bakhaidar, Rana B., Bahmdan, Rahaf H., Rizg, Waleed Y., Ali, Sarah A, Abdulaal, Wesam H., Nassar, Majed S., Alsuabeyl, Mohammed S., Alghaith, Adel F., Alshehri, Sultan, 2021. Oral gel loaded with penciclovir–lavender oil nanoemulsion to enhance bioavailability and alleviate pain associated with herpes labialis. Drug Delivery 28 (1), 1043–1054. https://doi.org/10717544.2021.1931561.

ICH, ICH Expert Working Group, 2005. International Conference on Harmonization (ICH) of Technical Requirements for the Registration of Pharmaceuticals for Human Use, Validation of Analytical Procedures: Text and Methodology, ICH-Q2(R1), 2005. Stat. Med. https://www.gmp-compliance.org/files/guidemgr/Q2(R1).pdf. (Accessed 24 november 2022).

Jantratid, E., Janssen, N., Reppas, C., Dressman, J.B., 2008. Dissolution Media Simulating Conditions in the Proximal Human Gastrointestinal Tract: An Update. Pharm Res 25, 1663. https://doi.org/10.1007/s11095-008-9569-4.

Javadzadeh, Y., Hamedeyazdan, S., 2012. Novel Drug Delivery Systems for Modulation of

Gastrointestinal Transit Time, in: Recent Advances in Novel Drug Carrier Systems. IntechOpen. 10.5772/50250.
Kansy, M., Senner, F., Gubernator, K., 1998. Physicochemical high throughput screening: parallel artificial membrane permeation assay in the description of passive absorption processes. J Med Chem 41, 1007–1010. https://doi.org/10.1021/jm970530e.
Koehl, N.J., Henze, L.J., Kuentz, M., Holm, R., Griffin, B.T., 2020. Supersaturated Lipid-Based Formulations to Enhance the Oral Bioavailability of Venetoclax. Pharmaceutics 12, 564. https://doi.org/10.3390/pharmaceutics12060564.
Kotschy, A., Szlavik, Z., Murray, J., Davidson, J., Maragno, A.L., Le Toumelin-Braizat, G., Chanrion, M., Kelly, G.L., Gong, J.-N., Moujalled, D.M., Bruno, A., Csekei, M., Paczal, A., Szabo, Z.B., Sipos, S., Radics, G., Proszenyak, A., Balint, B., Ondi, L., Blasko, G., Robertson, A., Surgenor, A., Dokurno, P., Chen, I., Matassova, N., Smith, J., Pedder, C., Graham, C., Studeny, A., Lysiak-Auvity, G., Girard, A.-M., Gravé, F., Segal, D., Riffkin, C.D., Pomilio, G., Galbraith, L.C.A., Aubrey, B.J., Brennan, M.S., Herold, M.J., Chang, C., Guasconi, G., Cauquil, N., Melchiore, F., Guigal-Stephan, N., Lockhart, B., Colland, F., Hickman, J.A., Roberts, A.W., Huang, D.C.S., Wei, A.H., Strasser, A., Lessene, G., Geneste, O., 2016. The MCL1 inhibitor S63845 is tolerable and effective in diverse cancer models. Nature 538, 477–482. https://doi.org/10.1038/nature19830.
Larsen, L., Lorimer, S.D., Perry, N.B., 2007. Contrasting chemistry of fruits and leaves of two Pseudowintera species: Sesquiterpene dialdehyde cinnamates and prenylated flavonoids. Biochem. Syst. Ecol. 35, 286–292. https://doi.org/10.1016/j.bse.2006.11.001.
Letai, A., Bassik, M.C., Walensky, L.D., Sorcinelli, M.D., Weiler, S., Korsmeyer, S.J., 2002. Distinct BH3 domains either sensitize or activate mitochondrial apoptosis, serving as prototype cancer therapeutics. Cancer Cell 2, 183–192. https://doi.org/10.1016/s1535-6108(02)00127-7.
Lipinski, C.A., Lombardo, F., Dominy, B.W., Feeney, P.J., 1997. Experimental and computational approaches to estimate solubility and permeability in drug discovery and development settings. Advanced Drug Delivery Reviews, In Vitro Models for Selection of Development Candidates 23, 3–25. https://doi.org/10.1016/S0169-409X(96)00423-1.
Ma, Z., Wang, N., He, H., Tang, X., 2019. Pharmaceutical strategies of improving oral systemic bioavailability of curcumin for clinical application. J Control Release 316, 359–380. https://doi.org/10.1016/j.jconrel.2019.10.053.
Ozogul, Y., Karsli, G.T., Durmuş, M., Yazgan, H., Oztop, H.M., McClements, D.J., Ozogul, F., 2022. Recent developments in industrial applications of nanoemulsions. Adv. Colloid Interface Sci. 304, 102685. https://doi.org/10.1016/j.cis.2022.102685.
Piazzini, V., Monteforte, E., Luceri, C., Bigagli, E., Bilia, A.R., Bergonzi, M.C., 2017. Nanoemulsion for improving solubility and permeability of Vitex agnus-castus extract: formulation and in vitro evaluation using PAMPA and Caco-2 approaches. Drug Deliv 24, 380–390. https://doi.org/10.1080/10717544.2016.1256002.
Ramsey, H.E., Fischer, M.A., Lee, T., Gorska, A.E., Arrate, M.P., Fuller, L., Boyd, K.L., Strickland, S.A., Sensintaffar, J., Hogdal, L.J., Ayers, G.D., Olejniczak, E.T., Fesik, S.W., Savona, M.R., 2018. A Novel MCL1 Inhibitor Combined with Venetoclax Rescues Venetoclax-Resistant Acute Myelogenous Leukemia. Cancer Discov 8, 1566–1581. https://doi.org/10.1158/2159-8290.CD-18-0140.
Rasmussen, M.L., Taneja, N., Neininger, A.C., Wang, L., Robertson, G.L., Riffle, S.N., Shi, L., Knollmann, B.C., Burnette, D.T., Gama, V., 2020. MCL-1 Inhibition by Selective BH3 Mimetics Disrupts Mitochondrial Dynamics Causing Loss of Viability and Functionality of Human Cardiomyocytes iScience 23, 101015.
Robert, A., Pujals, A., Favre, L., Debernardi, J., Wiels, J., 2020. The BCL-2 family protein inhibitor ABT-737 as an additional tool for the treatment of EBV-associated post-transplant lymphoproliferative disorders. Mol. Oncol. 14, 2520–2532. https://doi.org/10.1002/1878-0261.12759.
Ruchatz, F., Schuch, H., 1998. Physicochemical properties of Solutol® HS 15 and its solubilizates.
Séguy, L., Groo, A.-C., Goux, D., Hennequin, D., Malzert-Fréon, A., 2020. Design of Non-Haemolytic Nanoemulsions for Intravenous Administration of Hydrophobic APIs. Pharmaceutics 12, 1141. https://doi.org/10.3390/pharmaceutics12121141.
Séguy, L., Guyon, L., Maurel, M., Verdié, P., Davis, A., Corvaisier, S., Lisowski, V., Dallemagne, P., Groo, A.-C., Malzert-Fréon, A., 2021. Active Targeted Nanoemulsions for Repurposing of Tegaserod in Alzheimer's Disease Treatment. Pharmaceutics 13, 1626. https://doi.org/10.3390/pharmaceutics13101626.
Seiller, C., Maiga, S., Touzeau, C., Bellanger, C., Kervoëlen, C., Descamps, G., Maillet, L., Moreau, P., Pellat-Deceunynck, C., Gomez-Bougie, P., Amiot, M., 2020. Dual targeting of BCL2 and MCL1 rescues myeloma cells resistant to BCL2 and MCL1 inhibitors associated with the formation of BAX/BAK hetero-complexes. Cell Death Dis 11, 1–14. https://doi.org/10.1038/s41419-020-2505-1.
Shubber, S., Vllasaliu, D., Rauch, C., Jordan, F., Illum, L., Stolnik, S., 2015. Mechanism of mucosal permeability enhancement of CriticalSorb® (Solutol® HS15) investigated in vitro in cell cultures. Pharm Res 32, 516–527. https://doi.org/10.1007/s11095-014-1481-5.
Szlavik, Z., Csekei, M., Paczal, A., Szabo, Z.B., Sipos, S., Radics, G., Proszenyak, A., Balint, B., Murray, J., Davidson, J., Chen, I., Dokurno, P., Surgenor, A.E., Daniels, Z.M., Hubbard, R.E., Le Toumelin-Braizat, G., Claperon, A., Lysiak-Auvity, G., Girard, A.-M., Bruno, A., Chanrion, M., Colland, F., Maragno, A.-L., Demarles, D., Geneste, O., Kotschy, A., 2020. Discovery of S64315, a Potent and Selective Mcl-1 Inhibitor. J. Med. Chem. 63, 13762–13795. https://doi.org/10.1021/acs.jmedchem.0c01234.
Tron, A.E., Belmonte, M.A., Adam, A., Aquila, B.M., Boise, L.H., Chiarparin, E., Cidado, J., Embrey, K.J., Gangl, E., Gibbons, F.D., Gregory, G.P., Hargreaves, D., Hendricks, J.A., Johannes, J.W., Johnstone, R.W., Kazmirski, S.L., Kettle, J.G., Lamb, M.L., Matulis, S.M., Nooka, A.K., Packer, M.J., Peng, B., Rawlins, P.B., Robbins, D.W., Schuller, A.G., Su, N., Yang, W., Ye, Q., Zheng, X., Secrist, J.P., Clark, E.A., Wilson, D.M., Fawell, S.E., Hird, A.W., 2018. Discovery of Mcl-1-specific inhibitor AZD5991 and preclinical activity in multiple myeloma and acute myeloid leukemia. Nat Commun 9, 5341. https://doi.org/10.1038/s41467-018-07551-w.
United States Pharmacopeia, 2022. *Reagents, Simulated Gastric Fluid TS*. USP-NF. Rockville, MD: United States Pharmacopeia. https://doi.usp.org/USPNF/USPNF_XR3176_01_01.html. (Accessed 24 november 2022).
Veber, D.F., Johnson, S.R., Cheng, H.-Y., Smith, B.R., Ward, K.W., Kopple, K.D., 2002. Molecular properties that influence the oral bioavailability of drug candidates. J. Med. Chem. 45, 2615–2623. https://doi.org/10.1021/jm020017n.
Wang, X., Bathina, M., Lynch, J., Koss, B., Calabrese, C., Frase, S., Schuetz, J.D., Rehg, J.E., Opferman, J.T., 2013. Deletion of MCL-1 causes lethal cardiac failure and mitochondrial dysfunction. Genes Dev. 27, 1351–1364. https://doi.org/10.1101/gad.215855.113.
World Health Organization, 2018. The International Pharmacopeia, eight edition.